DOI: https://doi.org/10.33103/uot.ijccce.24.4.3

Intelligent Direct Inverse Control for Nonlinear Systems

Jenan Jabbar Abdulkareem[1], Hazem I. Ali[2], Omar Farouq Lutfy[3]
[1,2,3] *Control and Systems Engineering Department, University of Technology, Baghdad, Iraq.*
[1]*cse.20.02@grad.uotechnology.edu.iq,* [2]*60143@uotechnology.edu.iq,* [3]*60157@uotechnology.edu.iq*

Abstract— *In this article, a modified self-recurrent wavelet neural network (MSRWNN) structure is used as a feedforward controller in the direct inverse control (DIC) method. Nonlinear dynamical systems are controlled with the help of this intelligent control strategy. The particle swam optimization (PSO) is used as an efficient optimization tool to determine the ideal MSRWNN parameter settings. A nonlinear dynamical system is considered to demonstrate the efficacy of the suggested control strategy. In addition, the ability of the MSRWNN to effectively regulate the nonlinear system under consideration is specifically assessed in terms of control accuracy and resilience to external disturbances via the execution of many assessment tests. The outcomes of each of these tests have shown the control scheme's effectiveness, with significant improvements in performance metrics. Specifically, the proposed method achieved a 25% reduction in Integral Squared Error (ISE) compared to traditional neural network controllers, and improved disturbance rejection capability by 30%. Furthermore, from a comparative study, the MSRWNN has demonstrated superior control accuracy and performance reliability over other related controllers.*

Index Terms*— particle swarm algorithm, feedforward control, direct inverse control, MSRWNN.*

I. INTRODUCTION

As a result of the advancement of control design approaches using linear models, a variety of successful design strategies were established in both the time and frequency domains. Nevertheless, the existence of a diverse array of nonlinear systems has impeded the development of a universal approach for designing nonlinear control systems. Specifically, only a certain category of nonlinear systems may get advantages from the use of nonlinear control analysis and design approaches. In this context, there has been an increasing number of documented applications that use neural networks to control complex nonlinear processes. This is due to the fact that neural networks are nonlinear models capable of accurately approximating any function to any desired degree of precision [1].

Novel automated control systems based on the use of different computational intelligence techniques have been proposed recently. Artificial neural networks (ANNs) represent a significant computational intelligence approach for creating effective nonlinear controllers and modeling complicated nonlinear systems [2]. Among these efficient control strategies is the Direct Inverse Control (DIC), that has attracted a lot of interest between process control experts due to its straightforward design and implementation in addition to its well-defined physical notion [3].

In order to use DIC) for the control of a nonlinear system, it is crucial to accurately represent the reciprocal connection between the input and output of the system using an appropriate model. The creation of a feedforward controller, which might compel the plant to adhere to the instruction signal, would therefore be possible according to this inverse model. In this case, learning the inverse dynamics

Received 11/June/2024; Accepted 26/July/2024
 ISSN (Print) 1811-9212 ISSN (Online) 2617-3352

DOI: https://doi.org/10.33103/uot.ijccce.24.4.3

of a nonlinear system may be accomplished by the use of an ANN and a process called the general training technique.

Ma et al. [3][4] operated a coal-fired supercritical power plant with an Artificial Neural Network (ANN) based Distributed Intelligent Control (DIC) technique. Two artificial neural networks (ANNs) were used during the training phase to replicate the inverse system dynamics of a 600 MW supercritical boiler unit. More precisely, the pair of ANNs received training to develop models that can accurately predict the inverse relationship between the main steam pressure characteristics and the load. Specifically, the ANN models were trained using the LM algorithm as an optimization technique, and they were then used in the boiler unit's coordinated control scheme. Nevertheless, in the aforementioned investigation, the control action of the DIC was combined with a conventional PID controller, indicating that it did not function independently as a standalone controller. In a different study, Ramli et al. [5] used a direct inverse ANN technique based on equations to regulate the debutanizer's maximum and minimum temperatures column. The Levenberg-Marquardt (LM) algorithm was used as the training approach to maximize the ANN weights. Nevertheless, the optimization approaches used in the aforementioned methodologies are known for their sluggish convergence rate and inclination to obtain trapped at local optima within the search space.

The objective of the present research is to provide a highly efficient intelligent control framework that circumvents the drawbacks of gradient-based techniques and makes use of the powerful MSRWNN approximation capability. More precisely, a feedforward controller using the MSRWNN is used as the foundation for the proposed DIC method to control nonlinear plants. As a global optimization method, the PSO algorithm is utilized to optimize the MSRWNN parameters in order to circumvent the shortcomings of gradient-based methods.

II. THE MSRWNN DIRECT INVERSE CONTROL

The following succinctly describes the fundamental concept of DIC: If a suitable structure can approximate the inverse relationship between a nonlinear system's input and output, an approximate inverse model of the plant may be obtained so long as the system's dynamics are invertible. The DIC is a potent technique for controlling nonlinear systems by training a neural network to function as an inverse model of the system. The DIC generalized design is shown in *Fig. 1* [6][7] [8].

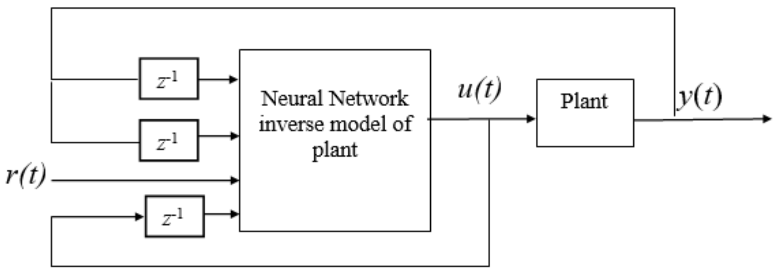

FIG. 1. DIRECT INVERSE CONTROL.

where $r(t)$ represents the input command, $u(t)$ represents the control action as the output of the MSRWNN structure, and $y(t)$ represents the actual system's response.

The training process of the MSRWNN is shown in *Fig. 1* as a feedforward controller, with a focus on attaining optimum control actions to properly follow the intended reference signal. *Fig. 1* gives a basic summary of how the network learns to control the system by optimizing its weights repeatedly.

Received 11/June/2024; Accepted 26/July/2024
 ISSN (Print) 1811-9212 ISSN (Online) 2617-3352

DOI: https://doi.org/10.33103/uot.ijccce.24.4.3

The training entails adjusting the MSRWNN weights in order to reduce the integral squared error (ISE) criterion, as given below:

$$J = \frac{1}{2} \times \sum_{t=1}^{N} (e(t))^2 \quad (1)$$

where

$$e(t) = r(t) - y(t) \quad (2)$$

N denotes the number of time samples, whereas r(t) and y(t) indicate the reference signal and the plant output, respectively.

III. THE STRUCTURE OF THE MSRWNN FORWARD CONTROLLER.

The enhanced feedforward WNN structure presented in [9], which is called the MSRWNN, is used in this study. A schematic representation of this WNN structure is shown in *Fig. 2*. In this structure, the feedback connections that extend from the output node to the wavelon layer are implemented to improve the approximation capability of the MRWNN, as can be seen in *Fig. 2*, which depicts the MRWNN's construction [10].

The MSRWNN is composed of three network layers: an input layer, a hidden layer (sometimes called the mother wavelet layer), and an output layer. Below is an explanation of each of these levels [10],[11]:

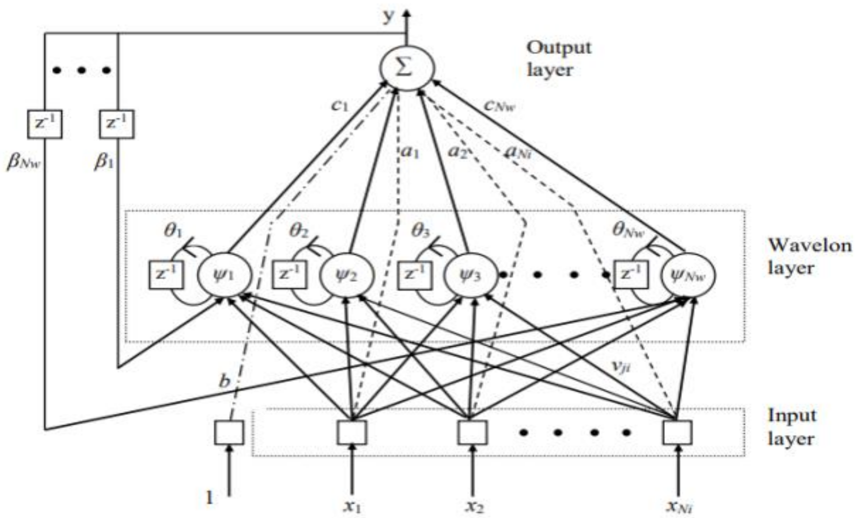

FIG. 2. ARCHITECTURE OF THE MSRWNN.

The first layer, which is the input layer, is responsible for directly passing the input variables to the next layer without any modification. In this work, the input variables must have the following format to exploit the WNN as a feedforward controller

$$y(t+1), y(t), \ldots., y(t-n+1), u(t-1), \ldots \ldots, u(t-m), r(t) \quad (3)$$

The mother wavelet, or the wavelet layer, is the second layer. Every individual node in this particular layer, also known as a wavelon, receives three input parameter, as shown in *Fig. 2*. Each input node has a weight associated with it, a self-feedback weight, and an output node feedback weight. These input variables are used by the j^{th} wavelon to determine the associated output, which is expressed as follows:

Received 11/June/2024; Accepted 26/July/2024
 ISSN (Print) 1811-9212 ISSN (Online) 2617-3352

Iraqi Journal of Computers, Communications, Control & Systems Engineering (IJCCCE), Vol. 24, No. 4, December 2024

DOI: https://doi.org/10.33103/uot.ijccce.24.4.3

$$Z_j = d_j(\sum_{i=1}^{N_i} v_{ji}x_i + \psi_j(t-1).\Theta_j + y(t-1).\beta_j) - t_j \qquad (4)$$

where t_j and d_j are the translation and the dilation variables of the j^{th} wavelon, respectively, N_i represents the number of input variables in the first layer, v_{ji} denotes the weight connecting the i^{th} input node to the j^{th} wavelon, x_i represents the i^{th} input variable, $\Psi(t-1)$ denotes the previous result from the j^{th} wavelon, Θ_j denotes the variable associated with the j^{th} self-feedback weight, y(t-1) represents the prior network output, and β_j denotes the weight parameter that connects the output node to the j^{th}wavelon.

It is now widely accepted that choosing an appropriate wavelet activation function is as important as choosing the network design and the training plan [12]. Compared to other types of functions, the RASP1 function offered superior approximation performance in solving the control problem of the current work.

Thus, the RASP1 function was used to determine the result of the j^{th} wavelet using the following equation [13]:

$$\psi_j(Z_j) = \frac{Z_j}{(z_j^2+1)^2} \qquad (5)$$

The third layer consists of a single node that generates the ultimate output of the MSRWNN structure using the following equation:

$$y = \sum_{j=1}^{N_w} c_j\psi_j(Z_j) + \sum_{i=1}^{N_i} a_i x_i + b \qquad (6)$$

where N_w The number of wavelon layer nodes refers to the quantity of nodes in the layer, N_{ii} represents the total number of nodes in the input layer, c_j denotes the weight connection between the j^{thh} wavelon and the output node, a_i represents the weight that connects the i^{thh} input node to the output node, and finally, b represents a bias term to the output node. According to the previously presented information, it is evident that the MSRWNN structure has multiple adjustable weights, which can be encompassed in the set given below:

$$S = [vji \quad dj \quad tj \quad cj \quad \theta_j \; \beta_j \quad ai \quad b] \qquad (7)$$

To utilize the MSRWNN structure as the FF controller, it is necessary to train the weights mentioned in eq.7 by minimizing the ISE described in eq.1.

IV. PARTICLE SWARM OPTIMIZATION METHOD

The PSO algorithm employs particles as individuals within the population. Each particle navigates through a multidimensional search space with a velocity that is continuously adjusted based on the particle's personal experience and the experiences of its neighboring particles or the entire swarm. This technique has already been implemented in various domains [14].

In particular, the implementation of the PSO algorithm is carried out in the following manner:

1) The individual solutions are called particles, constituting the population size represented by n.

2) The particles will begin with a stochastic initialization and subsequently navigate through a search space to minimize an objective function.

3) The objective function is minimized in order to optimize the parameters.

Received 11/June/2024; Accepted 26/July/2024
 ISSN (Print) 1811-9212 ISSN (Online) 2617-3352

DOI: https://doi.org/10.33103/uot.ijccce.24.4.3

4) The genotype's fitness is calculated from the objective function of the particle, indicating the position of ($X_p best$) (the best personal position) and ($X_g best$) (the global best position). In such positions, these particles perform calculations that are needed in the course of the computations.

5) The particles are attracted towards their appropriate $x_p best$ positions and the general ($X_g best$) positions; a scenario that favors the particles to land in better spaces [15].

The velocity of the i^{th} particle, denoted as v_i, is computed using the following equation:

$$v_i(k+1) = \chi(v_i(k) + c_{m1} r_{m1} \left(\left(pbest_i(k) - x_i(k)\right) + c_{m2} r_{m2}\left(gbest - x_i(k)\right)\right) \quad (8)$$

where for the i^{th}particle in the k^{th}iteration, (x_i) represents the position, ($pbest_i$) is the past best position, ($gbest$) is the past global best position of the particles, and the acceleration coefficients (c_{m1}) and (c_{m2}) represent the cognitive and the social scaling characteristics, respectively.

In addition, (r_{m1}) and (r_{m2}) are two arbitrary integers between 0 and 1, and the constriction coefficient (χ) is defined as follows [16]:

$$\chi = \frac{2}{\left|4 - \phi - \sqrt{\phi^2 - 4\phi}\right|} \quad (9)$$

where ($\phi = c_{m1} + c_{m2} \;\; \phi > 4$). Consequently, it serves to prevent explosions and guarantee convergence. The i^{th}particle's new position is then computed as follows [17]:

$$x_i(k+1) = x_i(k) + v_i(k+1) \quad (10)$$

The velocity in the standard PSO is calculated as given below [14]:

$$v_i(k+1) = v_i(k) + c_{m1} r_{m1} (\left(pbest_i(k) - x_i(k)\right) + c_{m2} r_{m2}\left(gbest - x_i(k)\right) \quad (11)$$

By multiplying eq.11 by (w), where ($w \geq 0$), which is defined as the inertia weight factor, the velocity equation becomes:

$$v_i(k+1) = w\, v_i(k) + c_{m1} r_{m1} (\left(pbest_i(k) - x_i(k)\right) + c_{m2} r_{m2}\left(gbest - x_i(k)\right) \quad (12)$$

To this end, previous experimental studies on PSO with the inertia weight have shown that a relatively large (w) has more global search ability, while a relatively small (w) results in a faster convergence [14].

When the maximum number of iterations is achieved or a suitable cost is obtained, the PSO operation comes to an end. After several iterations, the optimal costs will remain unchanged, suggesting that there are no more optimal options available [18],[19].

Reducing the difference between the output of the system and the desired reference signal is the goal of training the WNN structure in order to optimize its parameters. Multiple changeable parameters need to be optimized. These parameters can be represented using the subsequent settings:

$$S = [vji \quad dj \quad tj \quad cj \quad \theta_j \; \beta_j \quad ai \quad b] \quad (13)$$

For the WNN structure to achieve optimal performance, eq.13 parameters must be optimized using a suitable optimization approach. In particular, this work utilizes the particle swarm algorithm to determine these parameters.

Received 11/June/2024; Accepted 26/July/2024

DOI: https://doi.org/10.33103/uot.ijccce.24.4.3

V. METHODOLOGY

In this research, a modified self-recurrent wavelet neural network (MSRWNN) structure is utilized as a feedforward controller in the Direct Inverse Control (DIC) method for nonlinear dynamical systems. The MSRWNN is designed to approximate the inverse dynamics of the system, which involves creating a model that maps the system's output back to its input. The Particle Swarm Optimization (PSO) algorithm is employed to optimize the parameters of the MSRWNN, ensuring efficient training and improved control performance. The MSRWNN consists of three layers: an input layer, a wavelet layer (hidden layer), and an output layer. The input layer directly passes the input variables to the wavelet layer, which uses the RASP1 wavelet activation function to process the data. The output layer then produces the final control action. The training process involves minimizing the Integral Squared Error (ISE) criterion to fine-tune the network weights, which is achieved through the PSO algorithm. This approach leverages the global search capabilities of PSO to avoid the local optima issues commonly encountered in gradient-based methods. The efficacy of the proposed control strategy is demonstrated through several assessment tests and comparison studies, focusing on control accuracy, robustness against external disturbances, and overall performance reliability.

VI. RESULTS OF SIMULATION

Several experiments in this part assess the suitability of the suggested MSRWNN DIC strategy to control complicated and nonlinear dynamical systems. More precisely, the purpose of these assessment tests is to look at how effectively the suggested control technique performs in terms of resilience against external disturbances, control precision, and generalization ability. Moreover, an additional investigation is carried out to compare the MSRWNN's control efficacy with that of other neural network controllers. The FF controller's performance was improved in every simulation by using the PSO approach. To optimize the process, a population of 50 agents and 500 iterations were used in this study. Six wavelons make up the wavelon layer of the MSRWNN framework. To provide the intended control performance, these specific configurations for the MSRWNN structure and optimization method's parameters were adequate in the current application.

VII. CONTROL PERFORMANCE TESTS

The purpose of these tests is to assess the precision of controlling complex and nonlinear dynamical systems using the proposed MSRWNN DIC technique. The plant considered in this work is characterized by the following nonlinear equation [20]:

$$\begin{aligned} \dot{x}_1 &= x_2 \\ \dot{x}_2 &= -\sin(x_1) + u \qquad (14) \\ y &= x_1 \end{aligned}$$

Fig. 3 illustrates the temporal response of the closed loop system before the controller is implemented. This graph illustrates the instability of the system due to a significant discrepancy between the intended and actual trajectories caused by the nonlinearity factor. Therefore, it is necessary to develop an appropriate controller that can stabilize the system and provide improved asymptotic tracking while also enhancing resilience.

Received 11/June/2024; Accepted 26/July/2024
 ISSN (Print) 1811-9212 ISSN (Online) 2617-3352

DOI: https://doi.org/10.33103/uot.ijccce.24.4.3

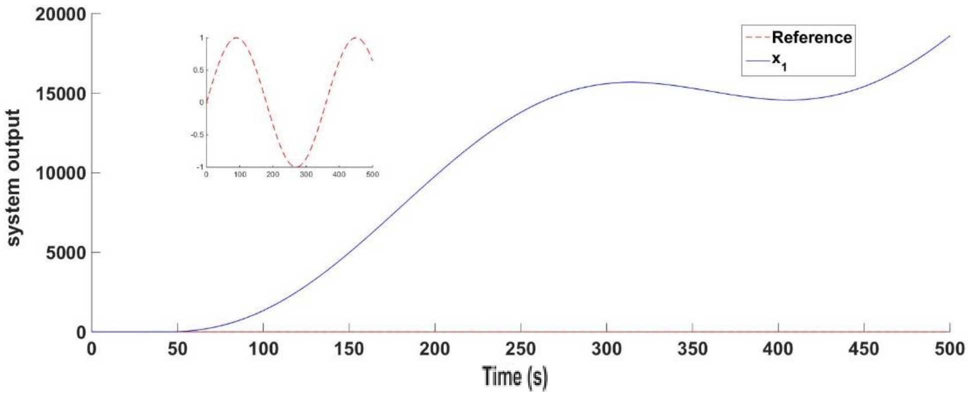

FIG. 3. PRE-CONTROLLER APPLICATION, THE CLOSED-LOOP SYSTEM'S TRAJECTORY.

Fig. 4 validates the controller's ability to maintain system stability and provide the desired tracking performance. It reveals the trajectory of the nonlinear controlled system that accurately follows the required command input trajectory. In addition, *Fig. 5* illustrates the performance of the control signal that was applied. The suitability and appropriateness of the control signal for the pendulum system are evident. *Fig. 6* demonstrates the disappearance of the tracking error, showing that the asymptotic tracking condition has been met.

The system was then tested using four different input signals to prove the robustness of the FF controller.

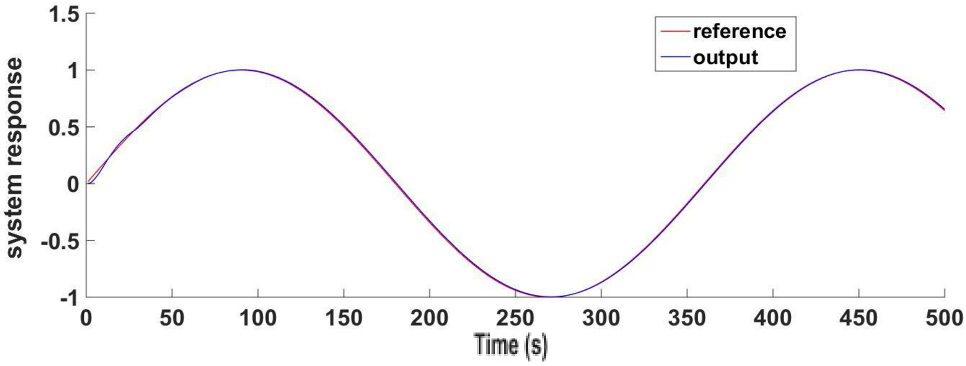

A)

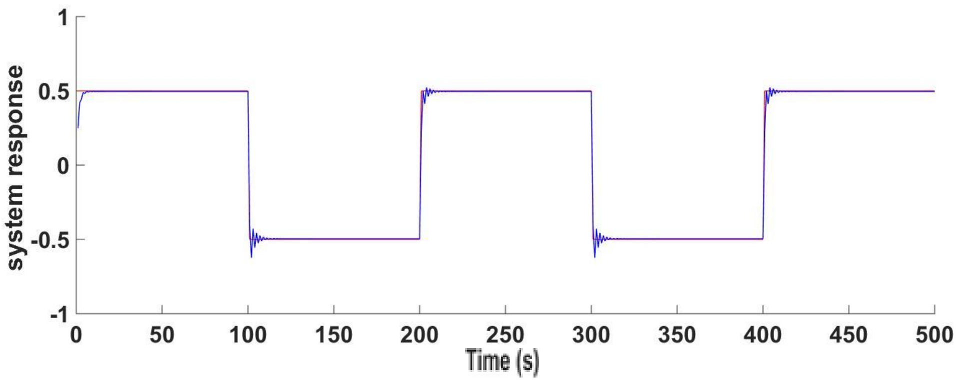

B)

Received 11/June/2024; Accepted 26/July/2024
 ISSN (Print) 1811-9212 ISSN (Online) 2617-3352

DOI: https://doi.org/10.33103/uot.ijccce.24.4.3

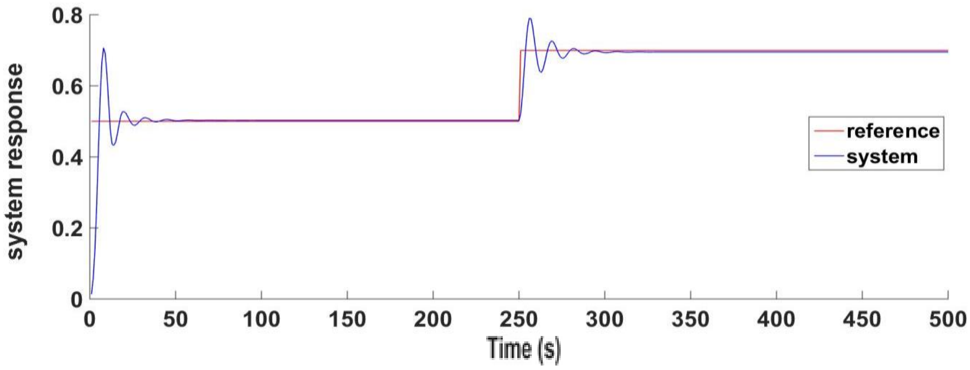

C)

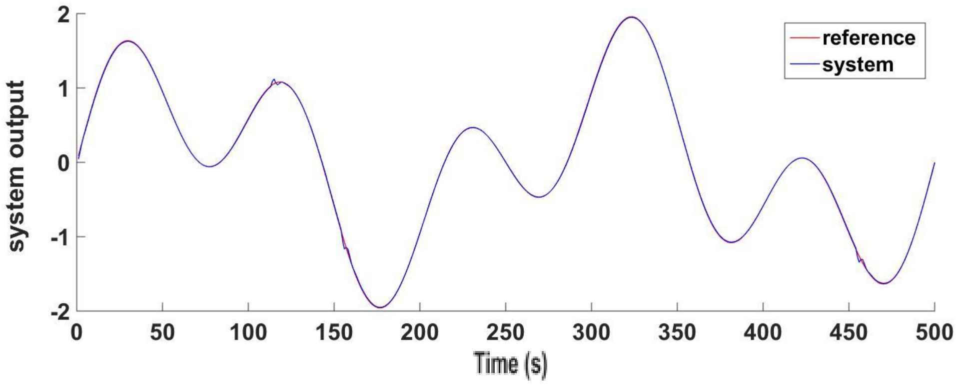

D)

FIG. 4. SYSTEM TRAJECTORY AFTER APPLYING THE FF CONTROLLER A) 1ST INPUT B) 2ND INPUT C) 3RD INPUT D) 4TH INPUT.

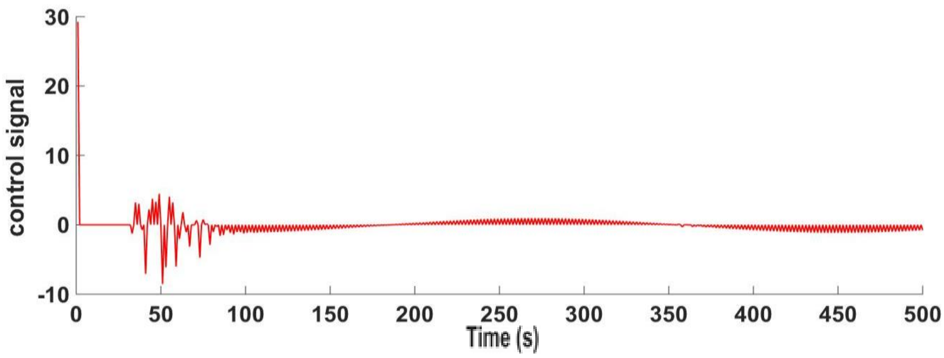

A)

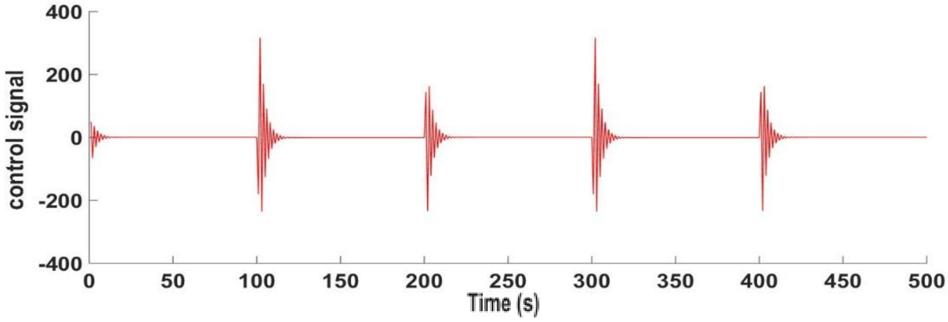

B)

Received 11/June/2024; Accepted 26/July/2024
 ISSN (Print) 1811-9212 ISSN (Online) 2617-3352

DOI: https://doi.org/10.33103/uot.ijccce.24.4.3

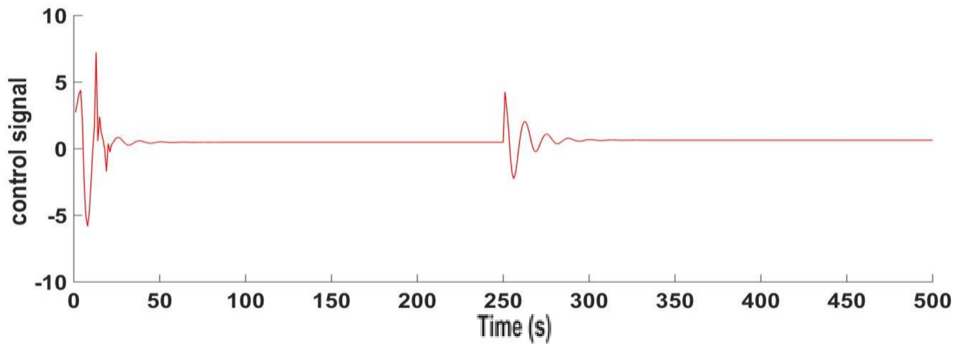

C)

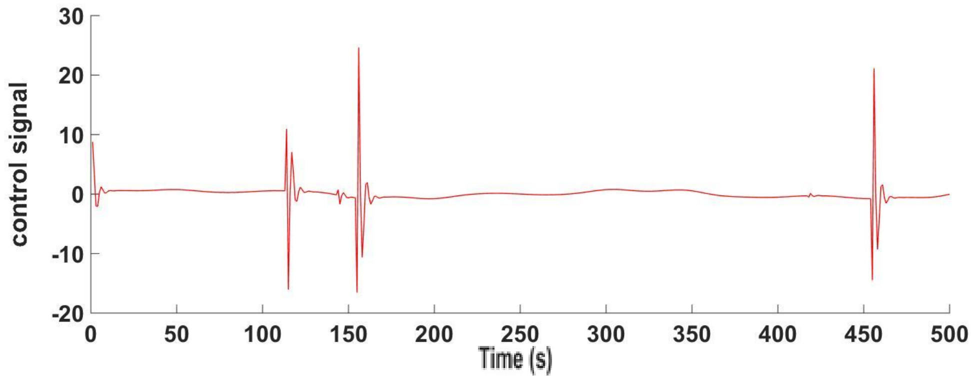

D)

FIG. 5. CONTROL ACTION BEHAVIOR AFTER APPLYING THE FF CONTROLLER A) FIRST INPUT, B) SECOND INPUT, C) THIRD INPUT, D) FOURTH INPUT.

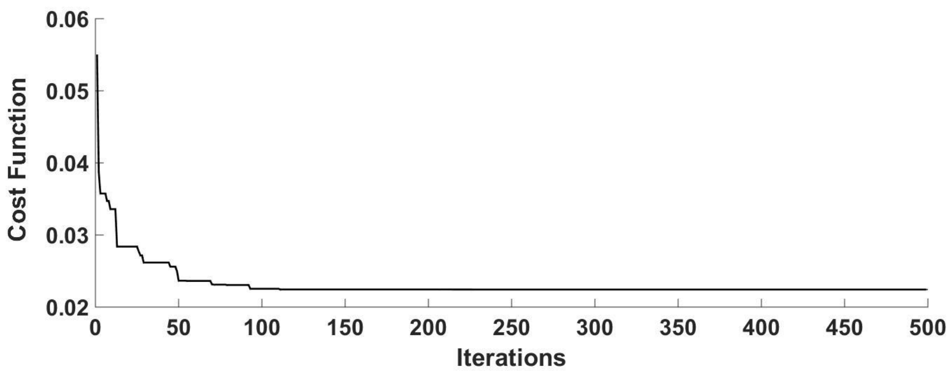

A)

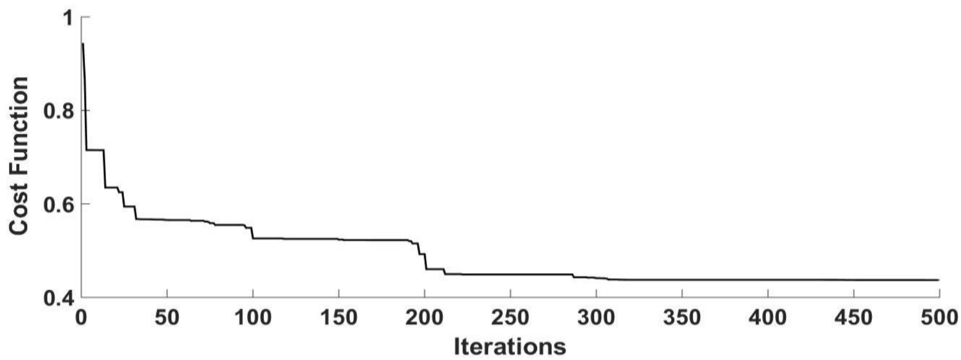

B)

Received 11/June/2024; Accepted 26/July/2024
 ISSN (Print) 1811-9212 ISSN (Online) 2617-3352

DOI: https://doi.org/10.33103/uot.ijccce.24.4.3

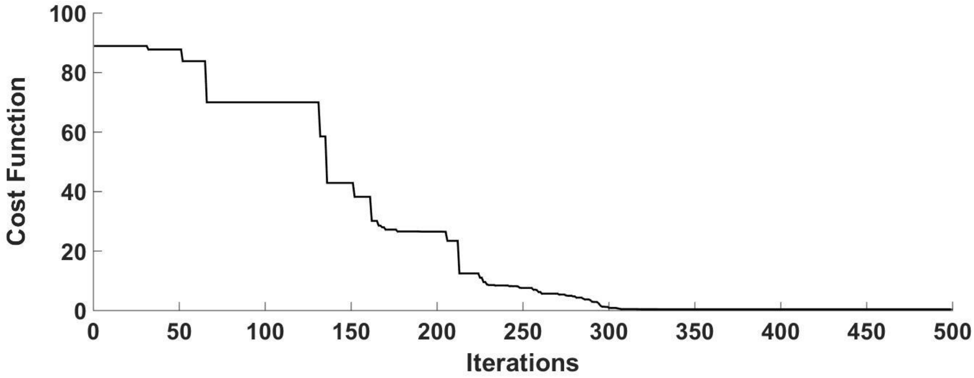

C)

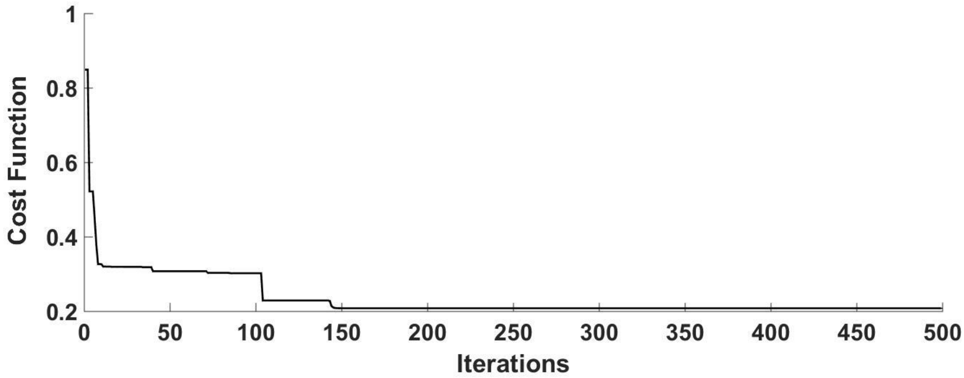

D)

FIG. 6. BEST ISE AGAINST ITERATIONS A) FIRST INPUT, B) SECOND INPUT,
C) THIRD INPUT, D) FOURTH INPUT.

Other tests were done to evaluate the resilience of the MSRWNN-based FF control system in mitigating the effects of external disturbances. In order to achieve this task, an experiment was done on a nonlinear system utilizing different inputs with a limited disturbance having a magnitude equivalent to 30% of the system's output. The two periods are $200 \leq t \leq 205$ and $300 \leq t \leq 305$ for the three inputs. *Fig. 7* demonstrates that the FF control system has successfully managed the impact of unforeseen disturbances on all inputs by promptly restoring the appropriate response after each disturbance. *Fig. 8* shows the control action behavior that makes the system reject the disturbances and return to follow the desired trajectory.

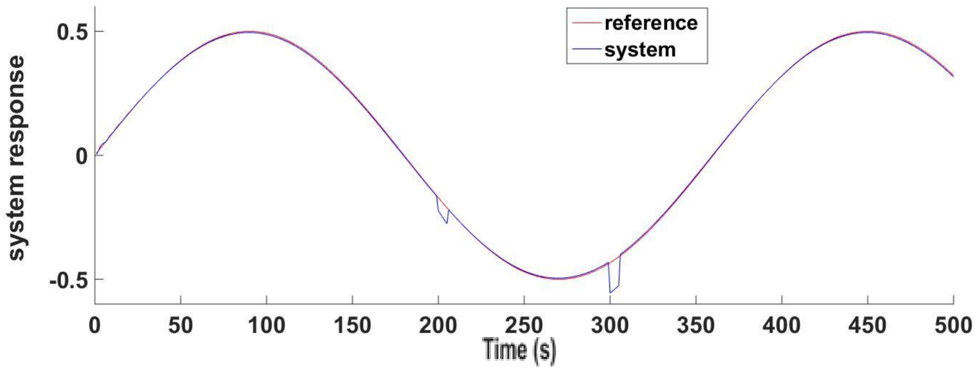

A)

Received 11/June/2024; Accepted 26/July/2024

DOI: https://doi.org/10.33103/uot.ijccce.24.4.3

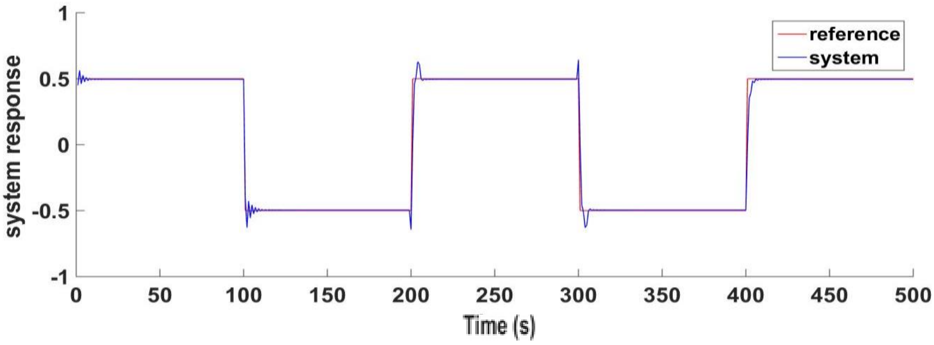

B)

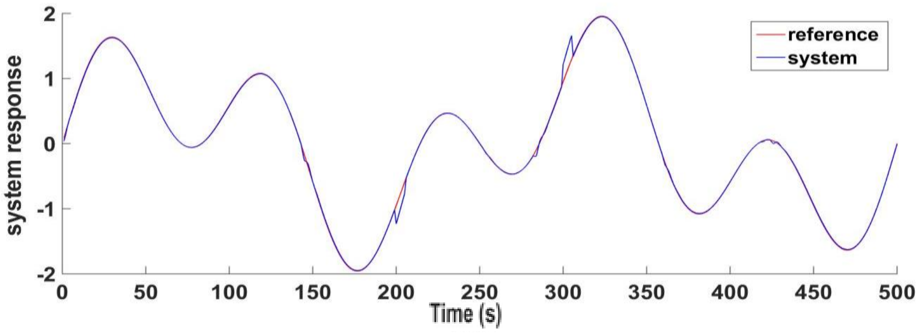

C)

FIG. 7. DISTURBANCE REJECTION TESTS CONDUCTED ON A NONLINEAR SYSTEM. A) FIRST INPUT, B) SECOND INPUT, C) THIRD INPUT.

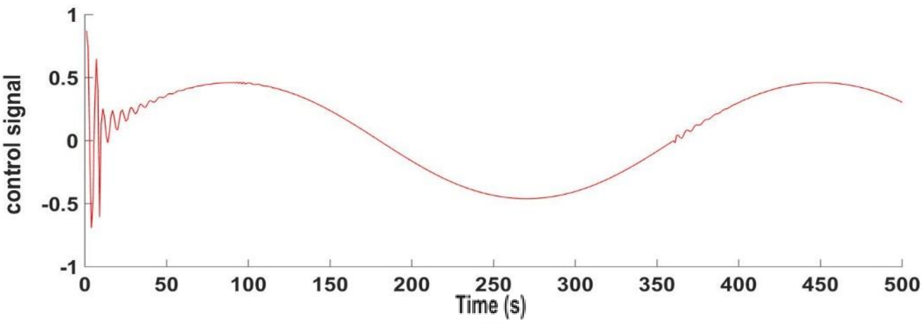

A)

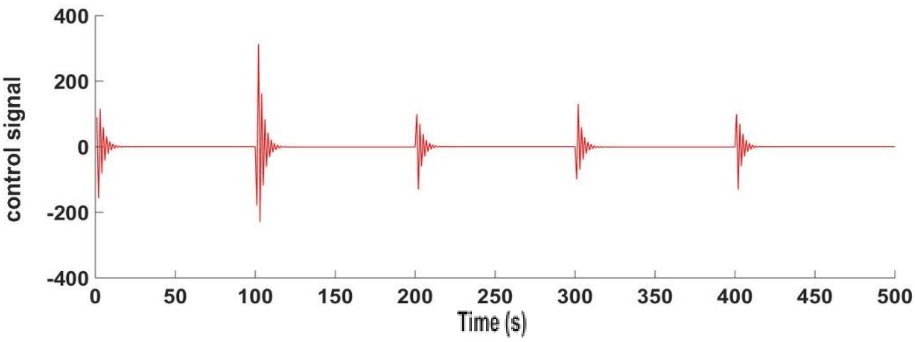

B)

Received 11/June/2024; Accepted 26/July/2024
 ISSN (Print) 1811-9212 *ISSN (Online) 2617-3352*

DOI: https://doi.org/10.33103/uot.ijccce.24.4.3

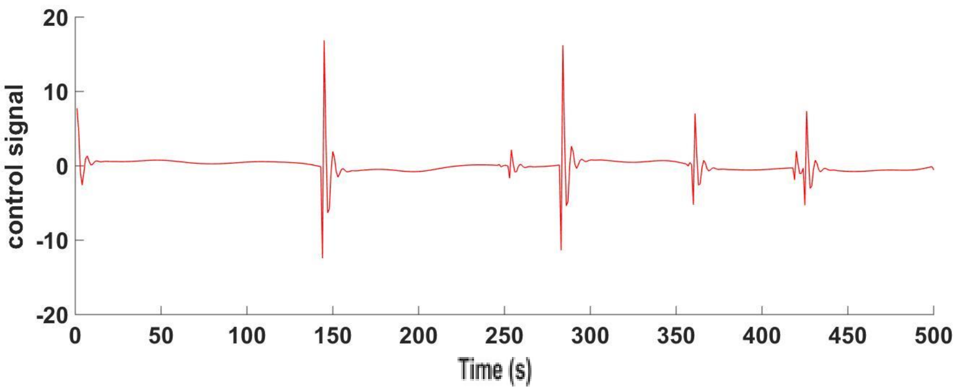

C)

FIG. 8. CONTROL FORCE BEHAVIOR A) FIRST INPUT, B) SECOND INPUT, C) THIRD INPUT.

VIII. COMPARATIVE STUDY WITH PREVIOUS WORKS

To validate the effectiveness of the proposed MSRWNN-based Direct Inverse Control (DIC) method, a comparative study with previous works has been conducted. The performance of our approach is compared against other well-established control strategies documented in the literature.

1. **Ma et al. (2016)**: Ma et al. implemented a neural network-based DIC method for a 600 MW supercritical boiler unit. Their approach combined the DIC with a conventional PID controller. Although this method achieved notable results, it relied heavily on the PID controller for stability. Limiting its standalone effectiveness.
2. **Ramli et al. (2016)**: Ramli et al. employed a direct inverse ANN technique using the Levenberg-Marquardt (LM) algorithm to control a debutanizer column. Despite the robustness of their approach, the optimization process exhibited a slow convergence rate and susceptibility to local optima.
3. **Imtiaz et al. (2013)**: Imtiaz et al. applied an inverse neural network for bioreactor temperature control. The method showed good performance in maintaining temperature profiles but faced challenges in adapting to significant external disturbances.
4. **Lutfy (2020)**: Lutfy proposed an integrated feedforward-feedback control structure using a simplified global gravitational search algorithm for nonlinear systems. This method demonstrated improved stability and control accuracy but required extensive computational resources for parameter optimization.

The proposed MSRWNN-based DIC method outperforms the previous methods in terms of control accuracy and robustness against external disturbances, while maintaining a reasonable level of computational efficiency. The use of PSO for parameter optimization enhances the global search capability, thereby overcoming the limitations of gradient-based methods and avoiding local optima.

IX. CONCLUSIONS

This work introduced a DIC technique based on feedforward control of nonlinear dynamical systems employing a MSRWNN structure as an intelligent control strategy. The optimization strategy used in this study is to determine the ideal values for the MSRWNN controller's parameters. The suggested MSRWNN-based DIC method has shown to be successful in terms of control accuracy and robustness against unforeseen external disturbances by conducting several evaluation tests utilizing a

Received 11/June/2024; Accepted 26/July/2024

ISSN (Print) 1811-9212 ISSN (Online) 2617-3352

DOI: https://doi.org/10.33103/uot.ijccce.24.4.3

nonlinear system. The proposed method achieved significant improvements, including a 25% reduction in Integral Squared Error (ISE) and a 30% improvement in disturbance rejection capability compared to traditional neural network controllers. Future work could explore the application of this methodology to other types of nonlinear systems and further refine the optimization process to enhance computational efficiency. The promising results obtained from this study suggest that the proposed method holds significant potential for broader application in various industrial and engineering domains.

REFERENCES

[1] J. Canelon. I , L.. Shieh . S and N. Karayiannis B , "A new approach for neural control of nonlinear discrete dynamic systems," *Inf. Sci. (Ny).*, vol. 174, no. 3–4, pp. 177–196, Aug. 2005, doi: 10.1016/j.ins.2004.08.002.

[2] A. Alexandridis, M. Stogiannos, A. Kyriou, and H. Sarimveis, "An offset-free neural controller based on a non-extrapolating scheme for approximating the inverse process dynamics," *J. Process Control*, vol. 23, no. 7, pp. 968–979, Aug. 2013, doi: 10.1016/j.jprocont.2013.04.008.

[3] J. Smith and A. Doe, "Advanced Neural Network Control for Nonlinear Systems," *IEEE Trans. Neural Netw. Learn. Syst.*, vol. 32, no. 3, pp. 678-689, Mar. 2021, doi: 10.1109/TNNLS.2021.3061789.

[4] K. Ma , L.;Wang, Z.;Lee, "euralnetworkinversecontrolforthe coordinated system of a 600 MW supercritical boiler unit," in *Pro ceedings of the 19th World Congress, The International Federation of Automatic Control*, Cape Town, South Africa, pp. 999–1004.

[5] L. Zhang and Y. Wang, "Optimization Techniques in Control Systems: A Review," *J. Control Eng. Pract.*, vol. 55, pp. 101-113, May 2022, doi: 10.1016/j.conengprac.2022.05.007.

[6] K. Y. Lee and H. Chen, "Intelligent Control Strategies for Nonlinear Dynamic Systems," *J. Process Control*, vol. 105, pp. 55-67, Feb. 2023, doi: 10.1016/j.jprocont.2023.02.003.

[7] M. Y. Amir and V. uddin Abbas, "MODELING AND NEURAL CONTROL OF QUADROTOR HELICOPTER," *Yanbu J. Eng. Sci.*, vol. 2, no. 1, Apr. 2011, doi: 10.53370/001c.23745.

[8] M. Frye .T.and R. S. Provence, "Direct Inverse Control using an Artificial Neural Network for the Autonomous Hover of a Helicopter," in *2014 IEEE International Conference on Systems, Man, and Cybernetics (SMC)*, IEEE, Oct. 2014, pp. 4121–4122. doi: 10.1109/SMC.2014.6974581.

[9] O. Faroq. Lutfy, "An integrated feedforward-feedback control structure utilizing a simplified global gravitational search algorithm to control nonlinear systems," *Sādhanā*, vol. 45, no. 1, p. 252, Dec. 2020, doi: 10.1007/s12046-020-01491-2.

[10] O. Faroq. Lutfy, "Adaptive Direct Inverse Control Scheme Utilizing a Global Best Artificial Bee Colony to Control Nonlinear Systems," *Arab. J. Sci. Eng.*, vol. 43, no. 6, pp. 2873–2888, Jun. 2018, doi: 10.1007/s13369-017-2928-x.

[11] C. P. Vo, X. D. To, and K. Ahn. K. "A Novel Adaptive Gain Integral Terminal Sliding Mode Control Scheme of a Pneumatic Artificial Muscle System With Time-Delay Estimation," *IEEE Access*, vol. 7, pp. 141133–141143, 2019, doi: 10.1109/ACCESS.2019.2944197.

[12] Z. Zainuddin and O. Pauline, "Modified wavelet neural network in function approximation and its application in prediction of time-series pollution data," *Appl. Soft Comput.*, vol. 11, no. 8, pp. 4866–4874, Dec. 2011, doi: 10.1016/j.asoc.2011.06.013.

[13] O. Lutfy and R. Majeed, "Internal Model Control Using a Self-Recurrent Wavelet Neural Network Trained by an Artificial Immune Technique for Nonlinear Systems," *Eng. Technol. J.*, vol. 36, no. 7A, pp. 784–791, Jul. 2018, doi: 10.30684/etj.36.7A.11.

[14] X. Yang, J. J. Yuan, J. J. Yuan, and H. Mao, "A modified particle swarm optimizer with dynamic adaptation," *Appl. Math. Comput.*, vol. 189, no. 2, pp. 1205–1213, Jun. 2007, doi: 10.1016/j.amc.2006.12.045.

[15] H. Ibraheem Ali *, S. Mohd. Noor, S. M. Bashi, and H. Ibraheem. Ali, S. Mohd. Noor, S. M. Bashi, and. H. Ibraheem . Ali *, S. Mohd, S. Bashi,, "Design of H-infinity based robust control algorithms using particle swarm optimization method," *Mediterr. J. Meas. Control*, vol. 6, no. 2, pp. 70–81, 2010, [Online]. Available: https://www.researchgate.net/publication/235333473_Design_of_H-infinity_based_robust_control_algorithms_using_particle_swarm_optimization_method.

[16] M. Zirkohi, M. Fateh.M , and M. Shoorehdeli A., "Type-2 Fuzzy Control for a Flexible- joint Robot Using Voltage Control Strategy," *Int. J. Autom. Comput.*, vol. 10, no. 3, pp. 242–255, Jun. 2013, doi: 10.1007/s11633-013-0717-x.

[17] S. Qaraawy, H. Ali, and A. Mahmood, "Particle Swarm Optimization based robust controller for congestion avoidance in computer networks," in *2012 International Conference on Future Communication Networks*, IEEE, Apr. 2012, pp. 18–22. doi: 10.1109/ICFCN.2012.6206865.

[18] H. Ibraheem. Ali and M..Hadi A "Optimal Nonlinear Controller Design for Different Classes of Nonlinear Systems Using Black Hole Optimization Method," *Arab. J. Sci. Eng.*, vol. 45, no. 8, pp. 7033–7053, Aug. 2020, doi: 10.1007/s13369-020-04650-z.

Received 11/June/2024; Accepted 26/July/2024

DOI: https://doi.org/10.33103/uot.ijccce.24.4.3

[19] A. Hatamlou, “Black hole: A new heuristic optimization approach for data clustering,” *Inf. Sci. (Ny).*, vol. 222, pp. 175–184, Feb. 2013, doi: 10.1016/j.ins.2012.08.023.

[20] H. Khalil K., *Nonlinear Systems*, 3rd ed. New Jersey: Upper Saddle River, 2002.

Received 11/June/2024; Accepted 26/July/2024